Acta Chemica Scandinavica, 1997: 51: 602–609
Printed in UK – all rights reserved

ACTA
CHEMICA SCANDINAVICA
ISSN 0904–213X

Investigation of Coulomb-coupled Radical Ion Pairs of Benzophenonetetracarboxylic Acid and Triethylamine by Laser Photolysis Fourier Transform Electron Spin Resonance†

J. Säuberlich, O. Brede and D. Beckert*

Max Planck Society, Research Unit 'Time Resolved Spectroscopy' at the University of Leipzig, Permoserstr. 15, D-04303 Leipzig, Germany

Säuberlich, J., Brede, O. and Beckert, D., 1997. Investigation of Coulomb-coupled Radical Ion Pairs of Benzophenonetetracarboxylic Acid and Triethylamine by Laser Photolysis Fourier Transform Electron Spin Resonance. – Acta Chem. Scand. 51: 602–609. © Acta Chemica Scandinavica 1997.

The photoreduction of benzophenone-3,3′,4,4′-tetracarboxylic acid (BPTC) with triethylamine in aqueous solution has been studied by means of Fourier transform electron spin resonance (FT-ESR) coupled with laser photolysis. The primary electron transfer from triethylamine to BPTC triplet generates solvent-separated radical ion pairs. In addition to the radical anion $BPTC^{-\cdot}$ in the free state, the radical anion $BPTC^{-\cdot}$ and the triethylamine radical cation $TEA^{+\cdot}$ in a Coulomb-coupled solvent-separated ion pair could be detected. All radicals observed were spin-polarized emissively by the CIDEP triplet mechanism. The spectroscopic parameters were determined of radical ions both in the free state and in complexed pairs.

The kinetics of bound and free radical anions $BPTC^{-\cdot}$, of the radical cation $TEA^{+\cdot}$ monitored over the nanosecond time range describe the lifetime of a radical ion pair complex stabilized by Coulomb attraction and by hydrogen bonding. The lifetime of the pairs is strongly controlled by the pH of the solution and is estimated to be $\tau_{RP}=0.02$–0.8 μs depending on the pH value.

The photophysics and photochemistry of aromatic ketones have been widely investigated by steady state methods and by time-resolved techniques such as laser photolysis with optical and ESR detection.[1–5] Whereas the optical methods are appropriate for the study of the kinetics of reaction mechanisms that have a high time resolution, the ESR techniques are unique in that they allow for an analysis of the structure of the intermediate species. By use of Fourier transform electron spin resonance spectroscopy (FT-ESR),[6,7] the time resolution could be extended to the nanosecond range with full spectral resolution. Furthermore, the FT-ESR technique improves the sensitivity of time resolved ESR.[8]

After photolytic excitation, the primary steps in the photoreduction of aromatic ketones by amines are intersystem crossing (ISC) to the triplet state, and fast electron transfer from the amine to the ketone triplet generating the ketone radical anion and the amine radical cation, respectively.[9] Since ISC of aromatic ketones is anisotropic for the different triplet states, the radical ions or radicals observed on the nanosecond and microsecond timescale are usually spin polarized by chemically induced dynamic electron spin polarization (CIDEP – triplet and/or radical pair mechanism).[8,9] Because of CIDEP effects, the temporal behavior of ESR spectra is more complicated but gives more information concerning the primary step of the electron transfer reaction as well as the interactions inside the solvent separated radical ion pair. The spin lattice relaxation time of the spin polarized triplet state represents an internal clock to quantify the rate constant of the electron transfer reaction with different amines,[9] while the rise time of the highly resolved FT-ESR spectra of the ketone radical anion describes the lifetime of the radical ion pair complex with strong Coulomb and magnetic interactions.[10] This sequence of reactions in the photoreduction of aromatic ketone triplets by aliphatic amines can be described by eqns. (1)–(5),[2,10,11] where BPTC is benzophenone-3,3′,4,4′-tetracarboxylic acid and TEA triethylamine.

Excitation and intersystem crossing:

$$BPTC_{So} \xrightarrow{h\nu} BPTC_{S1} \xrightarrow{ISC} BPTC_{T1}^{*} \qquad (1)$$

* To whom correspondence should be addressed.
† Lecture held at the 14th International Conference on Radical Ions, Uppsala, Sweden, July 1–5, 1996.

Spin lattice relaxation of spin-polarized triplet state:

$$BPTC_{T1}^{*} \xrightarrow{^3T_1} BPTC_{T1} \quad (2)$$

Electron transfer in encounter complex:

$$BPTC_{T1}^{*} + TEA \xrightarrow{k_{diff}} \{BPTC_{T1}^{*} \ldots TEA\}$$

$$\xrightarrow{k_{et}} \{BPTC^{-\cdot *} \ldots TEA^{+\cdot *}\} \quad (3)$$

Escape from the solvent-separated ion pair to free radical ions:

$$\{BPTC^{-\cdot *} \ldots TEA^{+\cdot *}\} \xrightarrow{k_{esc}} BPTC^{-\cdot *} + TEA^{+\cdot *} \quad (4)$$

Deprotonation of radical cation:

$$TEA^{+\cdot *} + H_2O \rightarrow Et_2N\text{–}C^{\cdot}HCH_3^{*} + H_3O^{+} \quad (5)$$

The radical anion of benzophenone is stable on a millisecond timescale, therefore the recombination reaction should not be considered here. The asterisk * denotes spin-polarized radicals.

Time resolved FT-ESR experiments have been performed to investigate the photoreduction of anthraquinone by triethylamine in various alcoholic solvents.[11] In these experiments the semiquinone radical anion could only be detected in the free radical state,[10,11] because the linewidth of the radicals inside the radical pair is too large to be detected by the conventional FT-ESR technique. The missing signal in the deadtime of the cavity ($\approx$100 ns) causes a deviation in the baseline, and therefore, weak broad lines cannot be quantitatively detected by this method. In order to improve the baseline all experimental spectra were extrapolated to the deadtime by the linear prediction singular value decomposition (LPSVD) method.[12–15] Recently, we have extended our data analysis program with the LPSVD method (linear prediction singular value decomposition[12–14]) to extrapolate the free induction decay to the deadtime of our FT-ESR spectrometer. Using this method we are able to detect FT-ESR signals with linewidths as large as 0.5 mT.

In the present paper we report on the photoreduction of benzophenone-3,3′,4,4′-tetracarboxylic acid by a tertiary amine (triethylamine) in aqueous solution as detected by laser photolysis FT-ESR measurements. In these experiments we could detect the radical anion of the benzophenone in the free state in solution and the benzophenone radical anion and the triethylamine radical cation inside radical ion pair complexes at the same time. The simultaneous measurement of both radical ions of the geminate pair generated by the primary electron transfer reaction characterizes the structure and kinetic behavior of the solvent-stabilized radical ion pair more precisely.

Experimental

Laser photolysis was performed with 308 nm radiation of an excimer laser (Lambda Physik, LPX 105ESC; energy: 10–15 mJ per pulse; pulse width 10 ns) for the FT-ESR measurements and with a Nd^{3+}:YAG laser using the fourth harmonic with 266 nm (Spectra Physics Inc., Quanta Ray GCR-11; energy: $<$10 mJ per pulse; pulse width 3 ns) for the laser flash experiments with optical detection. The jitter of the laser pulse in the FT-ESR experiments with external triggering could be measured as low as 2 ns.

FT-ESR spectra were recorded with an X-band home-built spectrometer described in detail in Ref. 11. The cavity used was the Bruker split-ring module ER 4118 X-MS-5W. The microwave pulse is generated by a fast ECL-PIN diode with a rise time of 4 ns and amplified by a 1 kW traveling wave tube amplifier A710/X (Logimetric, Inc.). The minimal pulse width of a $\pi/2$ microwave pulse is 16 ns. The software for device control, data acqusition and data analysis were developed in our institute. The LPSVD program is described elsewhere.[15] The equipment for optical absorption spectroscopy has been described previously.[16]

The experimental FT-ESR spectra are given in frequency units in relation to the spectrum centre where the *g*-values are adjusted to the *g*-value of the sulfite radical $SO_3^{-\cdot}$ with $g(SO_3^{-\cdot}) = 2.00316$.[17]

Materials. Benzophenone-3,3′,4,4′-tetracarboxylic dianhydride and triethylamine (all from Aldrich) were used without further purification. Water was delivered from an ultra-pure water system Milli-Q Plus (Millipore). In order to avoid solute depletion by accumulated laser excitation and enrichment of photolytic reaction products, the solutions were allowed to flow through the sample cell (quartz tube with an inner diameter of 1.5 mm) at a rate of approximately 1–2 ml min^{-1}. The flow system for the sample was constructed completely with glass tubing to ensure that oxygen did not diffuse into the sample solution between the bubbling vessel and the cavity. With this equipment we were able to remove oxygen to a concentration as low as 3×10^{-7} mol dm^{-3}.

Results

The optical spectrum of the benzophenone-3,3′,4,4′-tetracarboxylic acid triplet shows a strong optical absorbance at about 380 nm with a triplet lifetime $\tau_{TR} = 1.4$ µs. The kinetics of the triplet quenching are shown as a dependence on the triethylamine concentration in Fig. 1 and, from a Stern–Volmer plot, the rate constant [eqn. (3)] could be determined to be $k_{et} = 1 \times 10^9$ M^{-1} s^{-1}.

In Fig. 2 the FT-ESR spectrum of the radical anion $BPTC^{-\cdot *}$, obtained by complex Fourier transformation of the extrapolated free induction decay, is represented for a delay of 2 µs between laser excitation and detection pulse. This spectrum can be assigned to the free benzophenone-3,3′,4,4′-tetracarboxylic acid radical anion

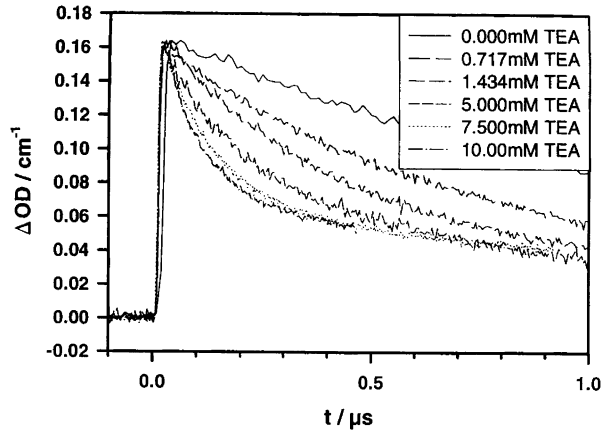

Fig. 1. Plots of absorbance at 380 nm of benzophenone-3,3',4,4'-carboxylic acid triplets generated by laser photolysis (10 mJ at 266 nm) as a dependence on triethylamine concentration (0.0–10 mM TEA).

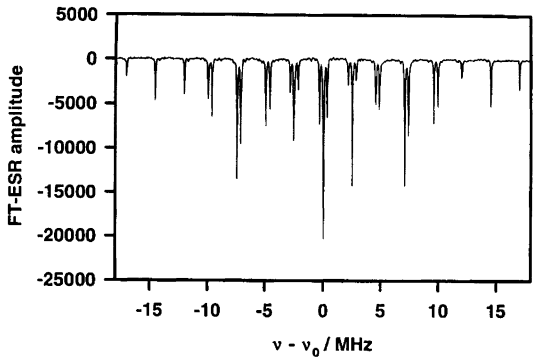

Fig. 2. FT-ESR spectra of radical anion $BPTC^{-\cdot}$* with a delay time $\tau_d = 2$ μs. The spectrum was calculated by Fourier transformation of the LPSVD extrapolated FID: sample, 1 mM benzophenone-3,3',4,4'-tetracarboxylic dianhydride with 30 mM triethylamine in water (pH = 11); number of repetitions, 100; acquisition time per point, 4 ns; number of points, 8K; laser energy per pulse, 15 mJ at 308 nm.

$BPTC^{-\cdot}$*. The hyperfine coupling constants, the *g*-value and the linewidth determined by simulation of the spectrum in Fig. 2 are listed in Table 1. The experimental spectrum in Fig. 2 provides no evidence for an additional radical in the field range considered.

An important problem in the quantitative analysis of time-resolved ESR spectra of geminate radical pairs is

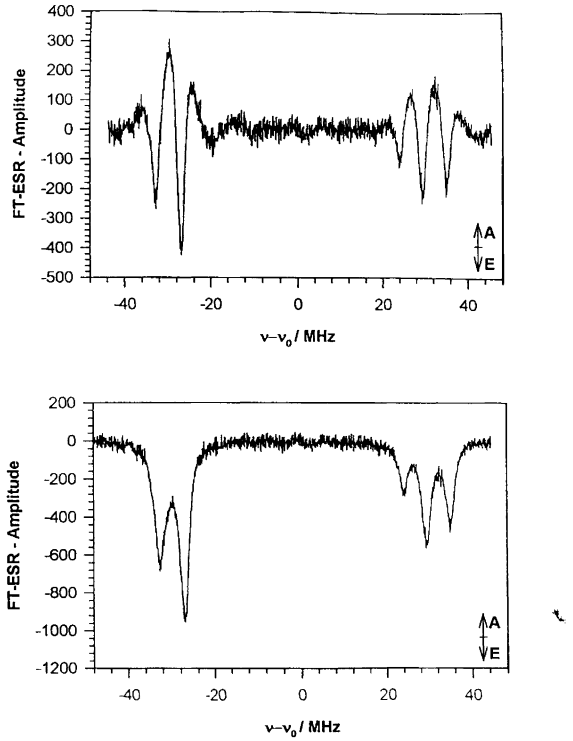

Fig. 3. Part of the FT-ESR spectrum of $TEA^{+\cdot}$ radical cation without (a) and with (b) extrapolation of the free induction decay by the LPSVD method. Sample and experimental conditions as in Fig. 2.

posed by the direct detection of both radicals of the pair. Up to now, only the radical anion of the radical ion pair $\{BPTC^{-\cdot}...TEA^{+\cdot}\}$ has been able to be detected.[10,11] The performance of the LPSVD method can be demonstrated on the FT-ESR spectra of the first two low-field line groups of $TEA^{+\cdot}$* shown in Fig. 3(a,b) with the zero-corrected FID (a) and the extrapolated FID (b). The spectra obtained show dispersive character without using the LPSVD method [Fig. 3(a)] and could not be analyzed quantitatively. After extrapolation of the FIDs to the deadtime, the spectra shown in Fig. 3(b) were obtained. The resulting FT-ESR spectrum of the two $TEA^{+\cdot}$* lines in Fig. 3(b) indicate the improved quantitative ESR results. The spectra are emissively polarized as is expected from the triplet CIDEP mechanism. With this improved method and the spectral parameters of the

Table 1. Spectroscopic parameters of $BPTC^{-\cdot}$ radical anion in the free state and paired state and of the $TEA^{+\cdot}$ radical cation in aqueous solution. The error limits are indicated in parentheses in units of the last digit.

Radical	*g*-Factor	Hfs coupling constants/MHz	Linewidth/kHz
$BPTC^{-\cdot}$	2.0035(6)	*a*(2 H,5,5') = 7.45(5)	
(free state and paired state)		*a*(2 H,2,2') = 7.09(5)	56 ± 3 (free state)
		a(2 H,6,6') = 2.51(5)	615 ± 30 (paired state)
$TEA^{+\cdot}$	2.0038(1)	*a*(N) = 56.0(1)	$(2.5 \pm 0.2) \times 10^3$
(^{14}N)		*a*(6 H, β) = 62.0(3)	
$TEA^{+\cdot}$	2.0038(0)	*a*(N) = 79.0(4)	$(2.5 \pm 0.2) \times 10^3$
(^{15}N)		*a*(6 H, β) = 62.0(0)	

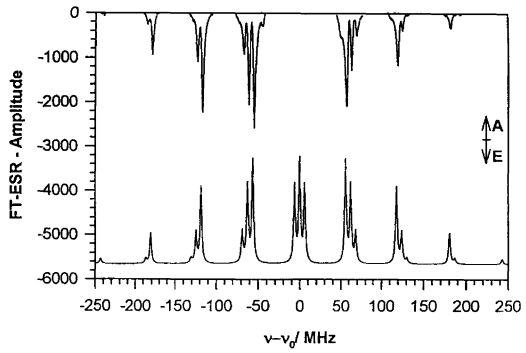

Fig. 4. FT-ESR spectrum of triethylamine radical cation $TEA^{+\cdot}$* at a delay time $\tau_d = 0.1$ μs. The individual groups were recorded separately with different offsets of B_0 and with repetition numbers of 1000 or more. With the simulated spectrum (bottom) the hyperfine coupling constants in Table 1 were calculated. The linewidth of the simulated spectrum is $\Delta B_{1/2} = 0.09$ mT.

radical cation $TEA^{+\cdot}$ from solid state experiments,[18,19] we could detect its time-resolved FT-EPR spectra in aqueous solution on a nanosecond timescale. The complete spectrum at a delay time of 0.1 μs is shown in Fig. 4. From the nine-line groups (21 lines in total) with a separation of 56.0 MHz we could detect six groups separately with a repetition number of 1000 or more. Because of the larger linewidth of the triethylamine radical cation $TEA^{+\cdot}$ the signal-to-noise ratio of the FID is rather low. The total intensity of all of the lines agrees with that for the benzophenone radical anion. From a simulation of the $TEA^{+\cdot}$ spectra, the hyperfine coupling constants and the *g*-value were determined (cf., the simulated spectrum in Fig. 4). The values obtained are listed in Table 1. In order to confirm the assignment of these line groups to the triethylamine radical cation we repeated the experiment using TEA marked with ^{15}N. The number of lines decreased as expected to 14 lines with a ^{15}N coupling constant of 79.0 MHz. The experimental spectrum at a delay time $\tau_d = 100$ ns is shown in Fig. 5. The hfs coupling constants for ^{15}N–$TEA^{+\cdot}$ determined from the simulated spectrum are listed in Table 1.

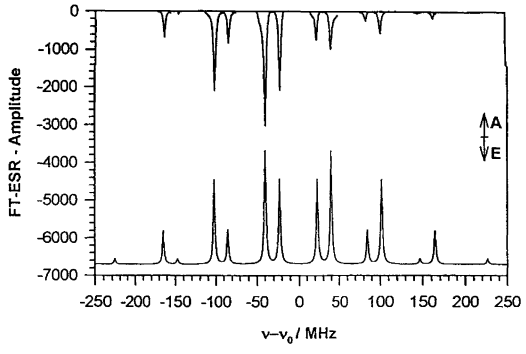

Fig. 5. FT-ESR spectrum of ^{15}N-triethylamine radical cation at delay time $\tau_d = 0.1$ μs. Experimental conditions as in Fig. 3. The hfs coupling constants in Table 1 were determined by simulation.

Because of the difference in the linewidth, the accuracy of the coupling constants and of the *g*-value is an order of magnitude lower for the radical cation $TEA^{+\cdot}$ than that of the radical anion $BPTC^{-\cdot}$.

From the experimental $BPTC^{-\cdot}$ spectra at pH = 11 for delay times shorter than 1 μs [Fig. 6(a,b)], it can be seen that, in addition to the sharp lines, each line group is superimposed with a broad background. These background lines appear at the same positions as the sharp line groups (deviation smaller than 5 μT) and their intensities decay quickly within the first microsecond. The influence of the central line group of the radical cation $TEA^{+\cdot}$* on the background signal can be eliminated using ^{15}N-labelled TEA because with $I(^{15}N) = 1/2$ no central line group appears. The intensity ratio of the small and broad $BPTC^{-\cdot}$ spectra was determined by superposition of two spectra with identical hfs constants but different linewidths. The results of these separations in a sharp and a broad line spectrum show that the linewidth of both lines could be fixed over the whole time range (48 ns to 4 μs). The linewidths obtained are (2.0 ± 0.1) μT for the small line and (22 ± 1) μT for the broad line.

The time dependence of these two intensities is depicted in Fig. 7. Whereas the ESR intensity of the small line spectrum (●) rises within the first microsecond, the broad line spectrum (▲) decays with the same time constant to first order. However, it is important to note here that the sum of the initial intensities of both spectra is smaller than the intensity of the small line spectrum in the maximum (about 50%) at 2 μs. From experiments in alcoholic solutions[10,11] it is known that the rise of the spin-polarized ESR intensity is caused by the escape-probability of the radical ions from solvent-separated radical ion pairs. Therefore, this rise time should be controlled by the pH of the solution. In Fig. 6(c,d) the same part of the radical anion spectrum as in Fig. 6(a,b) is shown at pH = 14. In these spectra the broad line background could be detected only at very short delay times ($\tau_d < 50$ ns). This means that the lifetimes of the solvent-separated radical ion pairs is shortened by more than one order of magnitude. Furthermore, the small line spectrum of the radical anion appears (ca. 80%) within the time constant of the signal detection channel (Fig. 7). Only about 20% of the radical anion ESR intensity rises with a time constant of 220 ns. These results require a two-phase process to be taken into account for the radical ion pair kinetics.

An alternative mechanism of the delayed build-up of the kinetics of the radical anion $BPTC^{-\cdot}$ is the involvement of secondary reaction channels. To prove this idea, the concentration of both reactants was varied. The variation of the triethylamine concentration enhances or diminishes the polarization factor of the radical anions by more effective electron transfer via reaction (3) than spin lattice relaxation $^3T_1$ of the spin-polarized triplet [eqn. (2)]. The reciprocal polarization factor of the radical anion vs. reciprocal triethylamine concentration is

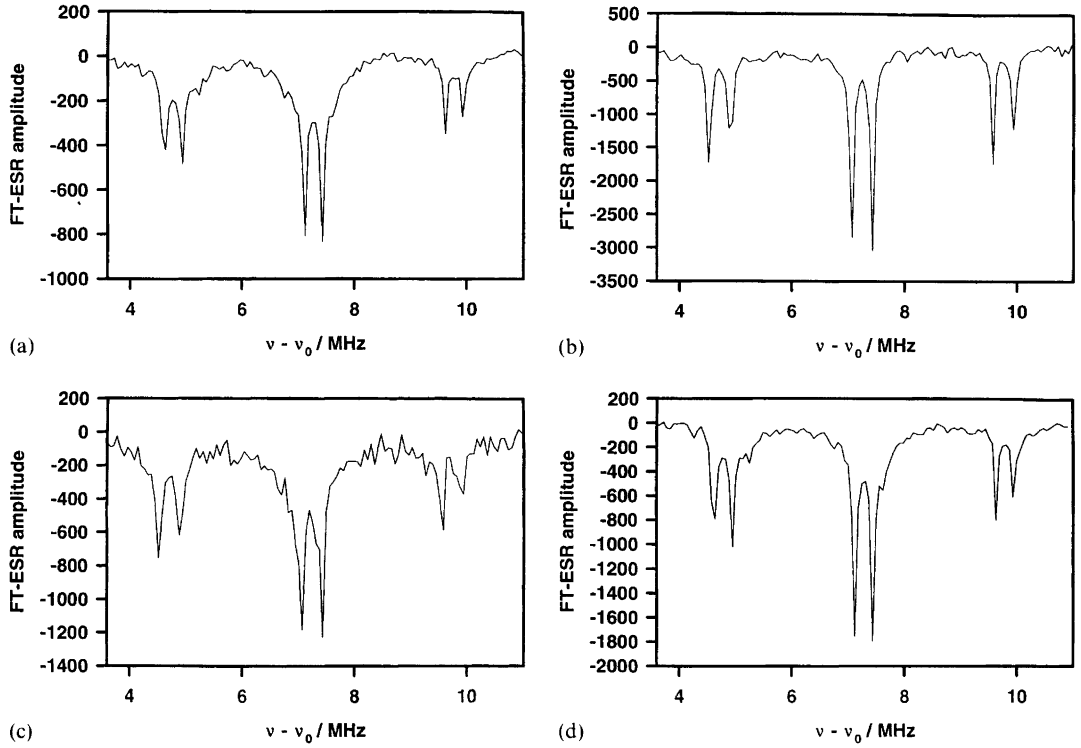

Fig. 6. Line groups at high frequency positions of the $BPTC^{-\cdot}$* FT-ESR spectrum at different delay times and pH-values: (a): $\tau_d = 0.2$ μs; pH = 11; (b): $\tau_d = 2.0$ μs; pH = 11; (c): $\tau_d = 0.2$ μs; pH = 14; (d): $\tau_d = 2.0$ μs; pH = 14.

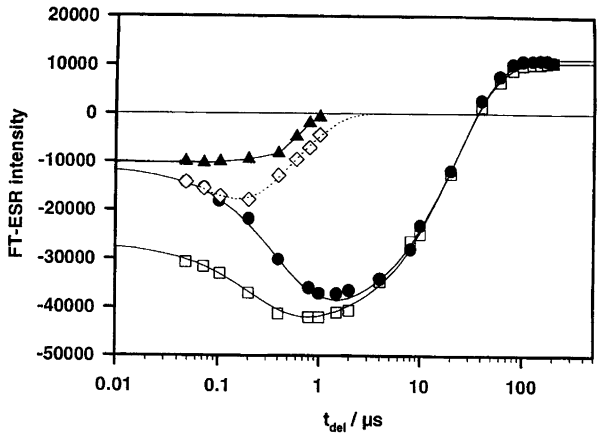

Fig. 7. Time dependence of the FT-ESR intensities of the $BPTC^{-\cdot}$* radical anion and the $TEA^{+\cdot}$ radical cation in the time range 48–200 μs.The intensities are normalized to the whole spectrum (line degeneracy and linewidth effects are included). Sample as in Fig. 2: ●, $BPTC^{-\cdot}$*, free state at pH = 11; ▲, $BPTC^{-\cdot}$*, pair state at pH = 11; □, $BPTC^{-\cdot}$*, free state at pH = 14; ◇, $TEA^{+\cdot}$*, pair state at pH = 11.

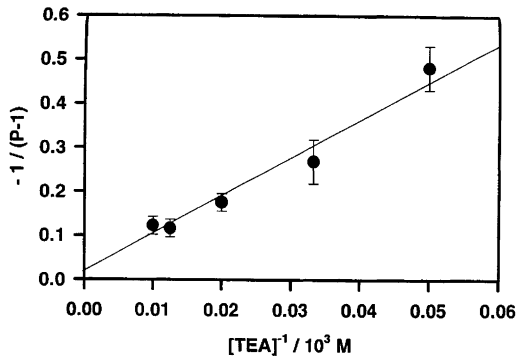

Fig. 8. Triplet polarization of $BPTC^{-\cdot}$* as a dependence on the triethylamine concentration. Competition between spin lattice relaxation of the BPTC triplet and the electron transfer reaction with triethylamine.

shown in Fig. 8. From the analysis of this plot using eqns. (2) and (3), the triplet polarization factor $P_T = -37$ and with the triplet quenching rate constant $k_{et} = 1 \times 10^9\ M^{-1}\ s^{-1}$ from the optical experiments (Fig. 1) a spin lattice relaxation time of $^3T_1 = 3.9$ ns could be deduced. At low TEA concentration the polarization pattern of the radical anion $BPTC^{-\cdot}$ shows a strong influence of radical pair polarization, but in Fig. 8 only the triplet polarization was considered. The radical pair polarization will be discussed in detail in a separate paper.

The variation of the concentration of benzophenone-3,3′,4,4′-tetracarboxylic acid changes the absorbance of the sample and therefore, the yields of triplets and of radical ions changes in the same way. In Fig. 9 the ESR intensities of $BPTC^{-\cdot}$ for different BPTC concentrations are presented as a dependence on the delay times τ_d. It is evident that the concentration of radical anions yields more light-absorbing molecules, but all four lines coincide after normalization with their Boltzmann magnetization. This means a secondary reaction of the triethylamine radical cation with benzo-

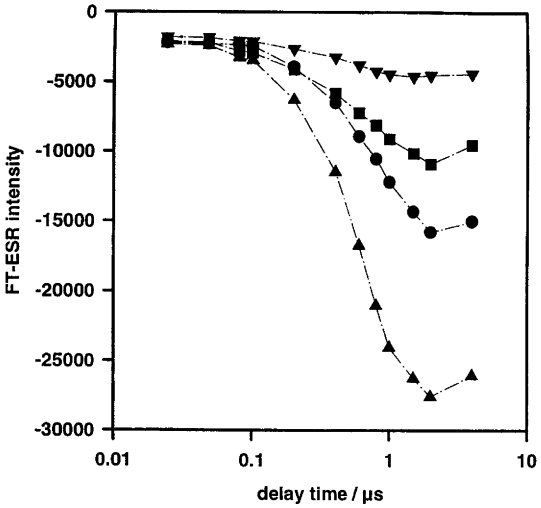

Fig. 9. Time dependence of the FT-ESR intensities of the $BPTC^{-\cdot}$* radical anions for different BPTC concentrations: ▼, 0.2 mM BPTC; ■, 0.5 mM BPTC; ●, 1.0 mM BPTC and ▲, 2.0 BPTC.

phenone-3,3′,4,4′-tetracarboxylic acid and the transfer of spin polarization from the radical cation to the radical anion can be excluded.

The kinetic analysis of the time dependence of the $BPTC^{-\cdot}$ ESR intensity $I(t)$ was carried out with a phenomenological function where the decay of the radical ion pairs and the spin lattice relaxation of the spin-polarized $BPTC^{-\cdot}$ radical anions are considered as independent processes, eqn. (6), where m_0 denotes that part

$$I(t) = \{(m_0 + m_1)[1 - \exp(-k_{esc}t)]\} \times [(P-1)\exp(-t/T_1) + 1] \quad (6)$$

of $BPTC^{-\cdot}$ that is generated with a fast time constant, m_1 that part which is build-up, with rate constant k_{esc} in first order, P the initial polarization of the radical anions and T_1 the spin lattice relaxation time of $BPTC^{-\cdot}$. The sum (m_0+m_1) represents the Boltzmann magnetization of $BPTC^{-\cdot}$. The lines in Fig. 7 were calculated with the parameter listed in Table 2. It should be noted that the escape rate constants k_{esc} observed in the ESR signals of $BPTC^{-\cdot}$ and $TEA^{+\cdot}$ from the radical ion pairs agree satisfactorily. Furthermore, the decay rate constant of the broad line spectrum has the same value within the error limits, whereas the escape rate constant at pH = 14 is larger by a factor of 3.

Table 2. Kinetic data for the radical anion $BPTC^{-\cdot}$* in the free and paired states and of the radical cation $TEA^{+\cdot}$*.

Radical	$m_0/(m_0+m_1)$	$k_{esc}/10^6\ s^{-1}$	$T_1/\mu s$
$BPTC^{-\cdot}$*/pH = 11 (free state)	0.14	1.2 ± 0.2	22 ± 2
$BPTC^{-\cdot}$*/pH = 14 (free state)	0.61	4.4 ± 0.3	22 ± 2
$BPTC^{-\cdot}$*/pH = 11 (paired state)	0.14	1.5 ± 0.4	
$TEA^{+\cdot}$*/pH = 11 (paired state)		1.5 ± 0.4	

The kinetics of the triethylamine radical cation were investigated with the line at field position $\Delta B \approx -120$ MHz from the center of the spectrum (Fig. 7). The ESR intensity of the emissive $TEA^{+\cdot}$* signal decays in the time range 50 ns to 1 µs. Apart from the first point at 50 ns no build-up kinetics could be detected and the relaxed equilibrium magnetization could not be measured in the absorptive mode at larger times (> 5 µs). Therefore, the calculation of a polarization factor of the radical cation $TEA^{+\cdot}$* is impossible. The decay kinetics of $TEA^{+\cdot}$* can be described by an exponential function with a time constant $\tau = (660 \pm 50)$ ns.

Discussion

As elucidated in the previous section to understand the FT-ESR data, we have to distinguish between three different radicals, two of which belong to the $BPTC^{-\cdot}$ radical anion and the third one to the triethylamine radical cation $TEA^{+\cdot}$. In the concentration range used (1 mM benzophenone-3,3′,4,4′-tetracarboxylic acid with 20–80 mM triethylamine in aqueous solution) the pH was 11 or higher in all samples. If we consider the two phenyl groups substituted with two carboxylic groups as independent in the dissociation properties we can use the results for the pK values from phthalic acid.[20] That means that from the four acidic protons, two are dissociated and two are free to form a hydrogen bridge between the two carboxy groups and with solvent water molecules.

The FT-ESR spectrum of $BPTC^{-\cdot}$ can be simulated by a triplet : triplet : triplet splitting with the coupling constants listed in Table 1. From this follows that both phenoxylic groups are symmetrical in their electronic structure with the same dissociation state and hydrogen bridged. The hyperfine coupling constants are in agreement with Ref. 21, where the ratio of coupling constants was related to spin density results and $a(5,5') > a(2,2') > a(6,6')$ was obtained. An additional coupling to the bridged protons could not be detected. The linewidth of 2.0 µT indicates a line narrowing by electron exchange processes but these effects were not investigated in more detail.

In the time range up to 1 µs an additional $BPTC^{-\cdot}$ spectrum with a larger linewidth was observed. The quantitative separation between the small and broad line spectra could be obtained only from LPSVD extrapolated FIDs with an exact, straight baseline of these spectra (cf., Fig. 2). The relative line positions of both spectra were determined with an accuracy in the order of 5 µT (cf., Fig. 6) and therefore the g-factor and hfs constants are equal in both spectra.

The line broadening may be caused by two different mechanisms: an unresolved additional hfs coupling, or by restricted molecular diffusional mobility combined with an additional magnetic interaction. An additional

hfs coupling might be produced by a hydrogen transfer reaction to the benzophenone triplet to generate a neutral ketyl radical. The hfs coupling constants of OH groups in alkyl or ketyl radicals are in the order of 0.03–0.08 mT in general, and depend strongly on the exchange rate of OH protons. In the case of fast hydrogen exchange of the OH group with the surrounding protons in the solution, the line splitting coalesces to a single line of linewidth $\Delta B_{1/2} = \tau_{ex}\gamma(\Delta B_O)^2$, where $\Delta B_{1/2}$ represents the experimental linewidth, ΔB_O the OH splitting constant and τ the time constant of the exchange process. With the values of $\Delta B_O = 0.05$ mT and $\Delta B_{1/2} = 0.005$ mT (pH = 11) the exchange time constant could be estimated as $\tau_{ex} = 5 \times 10^{-8}$ s. In order to check this interpretation the proton concentration of the solution was reduced by two orders of magnitude. As a result the linewidth of the broad background signal did not change at very short delay times ($\tau_d < 50$ ns). These two results, the rather large value of the exchange time constant and the independence of the linewidth on proton concentration reveals that the broad background spectrum cannot be attributed to ketyl radicals with an unresolved OH coupling.

The kinetic behavior of the small line radical anion spectrum has been interpreted in terms of the escape process of $BPTC^{-\cdot}$* from solvent-separated radical ion pairs.[10] Because of strong magnetic interactions in solvent-separated radical ion pairs in alcoholic solutions used in Refs. 10 and 11 the FT-ESR spectra of the radical ions of the pair could not be detected. Here, it was found that the lifetime of the radical ion pairs is larger in nonpolar solvents than in polar solvents. This effect can be explained by different shielding forces of solvent molecules. Furthermore, it was shown in Ref. 11 that the decay of the solvent-separated radical ion pairs could be described by a two-phase process, where the fast decay with a time constant of several tens of nanoseconds depends on the amine concentration. In the experiments presented here water was used as the solvent. The shielding effect of water molecules on the interactions in radical ion pairs should be larger than in alcoholic solvents. Therefore, we can also expect the magnetic interactions in radical ion pairs to be smaller and the linewidth in FT-ESR spectra to decrease in comparison with alcoholic solutions. These arguments suggest that the broad line background spectra are due to the $BPTC^{-\cdot}$ radical anion inside the solvent-separated radical ion pair. The spectroscopic parameters (*g*-factor, hyperfine coupling constants) are identical and the signals appear in emission as expected. To our knowledge, this is the first simultaneous detection of a radical ion in the paired state as well as in the free state in solution.

The build-up kinetics of $BPTC^{-\cdot}$* can also be described by a two-phase process. The ratio of fast-to-slow decay of the radical ion pairs depends on the pH of the solution. This behavior is similar to the base-catalyzed decay of radical ion pairs in alcoholic solutions described in Ref. 11.

The spectrum of the radical cation $TEA^{+\cdot}$* appears completely in emission in agreement with the CIDEP triplet mechanism. The polarization factor of $TEA^{+\cdot}$* could not be determined quantitatively because only a weak $TEA^{+\cdot}$ signal could be detected at large delay times (signal-to-noise ratio < 25 : 1 with the number of repetitions = 1000 and LPSVD extrapolation). With the polarization factor derived from the small line $BPTC^{-\cdot}$* spectrum of $P = -37$ we can deduce the signal-to-noise ratio of the Boltzmann-equilibrated $TEA^{+\cdot}$ spectrum to be < 1 : 1. Such a small signal of linewidth 0.1 mT cannot be quantitatively analyzed under our experimental conditions. Thus the intensity of the spin-polarized radical cation $TEA^{+\cdot}$* could be monitored on the timescale of a few microseconds only. The decay time ($\tau = 0.66$ μs) obtained agrees with the decay time of the $BPTC^{-\cdot}$ broad line spectrum and also with the rise time of the $BPTC^{-\cdot}$ small line spectrum. This confirms the interpretation that the $BPTC^{-\cdot}$ broad line spectrum and $TEA^{+\cdot}$* spectrum are due to solvent-separated radical ion pairs. With the decay time we have a direct measurement of the lifetime of ion-pair. Up to now the experiments give no information about the fate of $TEA^{+\cdot}$ at longer times. We hope to improve the detection conditions to increase the sensitivity for low-intensity broad-line spectra.

Conclusions

In this paper the photoreduction of benzophenone-3,3′,4,4′-tetracarboxylic acid by triethylamine in aqueous solution has been investigated. With electron transfer as the primary reaction step, solvent-separated radical ion pairs are generated. With our FT-ESR technique improved by LPSVD signal analysis, we are able to measure the spectra of free $BPTC^{-\cdot}$, pair-bound $BPTC^{-\cdot}$ and pair-bound $TEA^{+\cdot}$ with linewidths of $\Delta B_{1/2} = 0.2$, 2.2 and 90 μT, respectively. The *g* factor and the hyperfine coupling constants of $BPTC^{-\cdot}$ do not change in the paired state and agree well with the values of free-state $BPTC^{-\cdot}$. In addition to the line-broadening effects, knowledge of the kinetic behavior is essential in the assignment of the three spectra to the free and Coulomb-coupled paired state. The decay time constants of the paired state radicals agree reasonably well with the rise time of small line $BPTC^{-\cdot}$ * spectrum, which we attribute to $BPTC^{-\cdot}$ free in solution with a lifetime in the millisecond range. Therefore, the kinetics of all of the radical ions monitored describe the lifetime (τ_{Pair} = 0.6–0.8 μs) of the solvent-separated radical ion pairs.

Acknowledgment. Financial support for this work was provided by the *Deutsche Forschungsgemeinschaft*, by the *Fonds der Deutschen Chemischen Industrie* and by the *Sächsische Ministerium für Wissenschaft und Kultur.*

References

1. Scaiano, J. C. *J. Photochem. 2* (1973) 81.
2. Cohen, S. G., Parola, A. and Parsons, G. H. *Chem. Rev. 73* (1973) 141.
3. Sakaguchi, Y. and Hayashi, H. *Photochem. Photobiol. A: Chem. 65* (1992) 183.
4. Devadoss, C. W. and Fessenden, R. W. *J. Phys. Chem. 95* (1991) 7253.
5. Kavarnos, G. J. and Turro, N. J. *Chem. Rev. 86* (1986) 401.
6. Bowman. M. K. In: Kevan, L. and Bowman, M. K., Eds., *Modern Pulsed and Continous-wave Electron Spin Resonance,* Wiley, New York 1990, Chap. 1.
7. van Willigen, H., Levstein, P. R. and Ebersole, M. H. *Chem. Rev. 93* (1993) 173.
8. McLauchlan, K. A. In: Hoff, A. J., Ed., *Advanced EPR: Application in Biology and Biochemistry*, Elsevier, Amsterdam 1989, Chap. 10.
9. Beckert, D. and Schneider, G. *Chem. Phys. 116* (1987) 421.
10. Beckert, D., Plüschau, M. and Dinse, K. P. *J. Phys. Chem. 96* (1992) 3193.
11. Kausche, T., Säuberlich, J., Trobitzsch, E. and Beckert, D. *Chem. Phys. 208* (1996) 375.
12. Säuberlich, J. and Beckert, D. *J. Phys. Chem. 99* (1995) 12520.
13. deBeer, R. and van Ormondt, D., In: Hoff, A. J., Ed., *Advanced EPR: Application in Biology and Biochemistry*, Elsevier, Amsterdam 1989, Chap. 4.
14. Stephenson, D. S. *Prog. NMR Spectrosc. 20* (1988) 515.
15. Säuberlich, J. *Ph.D. Dissertation*, Leipzig (1996).
16. Zubarev, V. and Brede, O. *J. Chem. Soc., Perkin Trans. 2* (1994) 1821.
17. Jeevarajan, A. S. and Fessenden, R. W. *J. Phys. Chem. 93* (1989) 3511.
18. Lefkowitz, S. M. and Trifunac, A. D. *J. Phys. Chem. 88* (1984) 77.
19. Eastland, G. W., Ramakrishna Rao, D. N. and Symons, M. C. R. *J. Chem. Soc., Perkin Trans. 2* (1984) 1551.
20. Neta, P. and Fessenden, R. W. *J. Phys. Chem. 77* (1973) 620.
21. Rieger, P. H. and Fraenkel, G. K. *J. Chem. Phys. 37* (1962) 2811.